Electronic Supplementary Material (ESI) for Physical Chemistry Chemical Physics.

Supporting information

Utilization of DNA and 2D Metal Oxide interaction for optical biosensor

Partha Kumbhakar[a §], Indrani Das Jana[b §], Subhadip Basu [c §], Sandip Mandal[c], Saptarshi Banerjee[b], Subhanita Roy[b], Chinmayee Chowde Gowda[d], Anyesha Chakraborty[d], Ashim Pramanik[a,e], Pooja Lahiri[f], Basudev Lahiri[g], Amreesh Chandra[h], Pathik Kumbhakar[e], Arindam Mondal[b*], Prabal K Maiti[c*], Chandra Sekhar Tiwary[a*]

[a]Department of Metallurgical and Materials Engineering, Indian Institute of Technology Kharagpur, Kharagpur 721302, India
[b]School of Bioscience, Indian Institute of Technology Kharagpur, Kharagpur 721302, India
[c]Centre for Condensed Matter Theory, Department of Physics, Indian Institute of Science, Bangalore 560012, India
[d]School of Nano Science and Technology, Indian Institute of Technology Kharagpur, Kharagpur 721302, India
[e]Nanoscience Laboratory, Department of Physics, National Institute of Technology Durgapur, 713209, India.
[f]School of Medical Science and Technology, Indian Institute of Technology Kharagpur, Kharagpur 721302, India
[g]Department of Electronics and Electrical Communication Engineering, Indian Institute of Technology Kharagpur, Kharagpur 721302, India
[h]Department of Physics, Indian Institute of Technology Kharagpur, Kharagpur 721302, India

§-Equal contribution.

*E-mail: arin.cal@gmail.com, maiti@iisc.ac.in, chandra.tiwary@metal.iitkgp.ac.in.

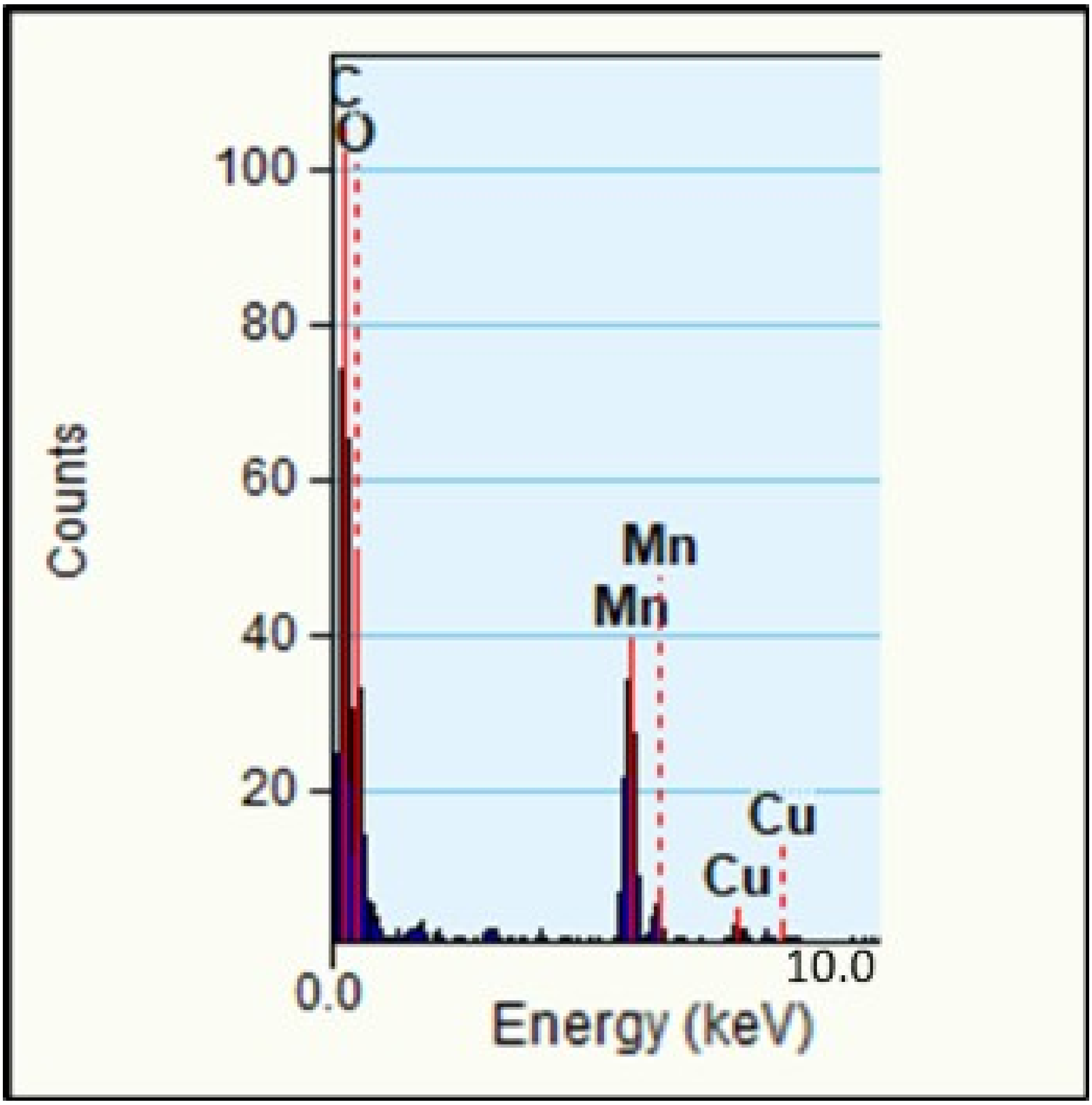

Fig. S1 EDX spectra of Mn_3O_4.

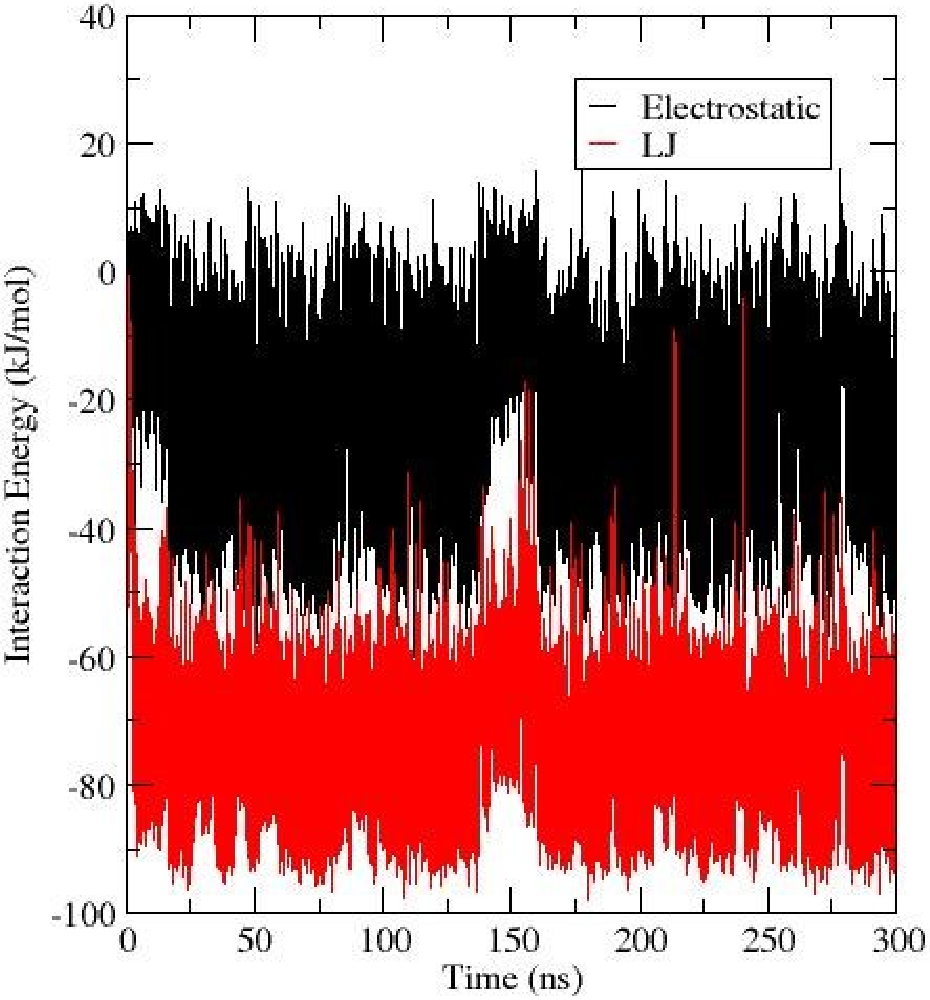

Fig. S2: Temporal evolution of interaction between 5'-guanine and Mn_3O_4 surface.

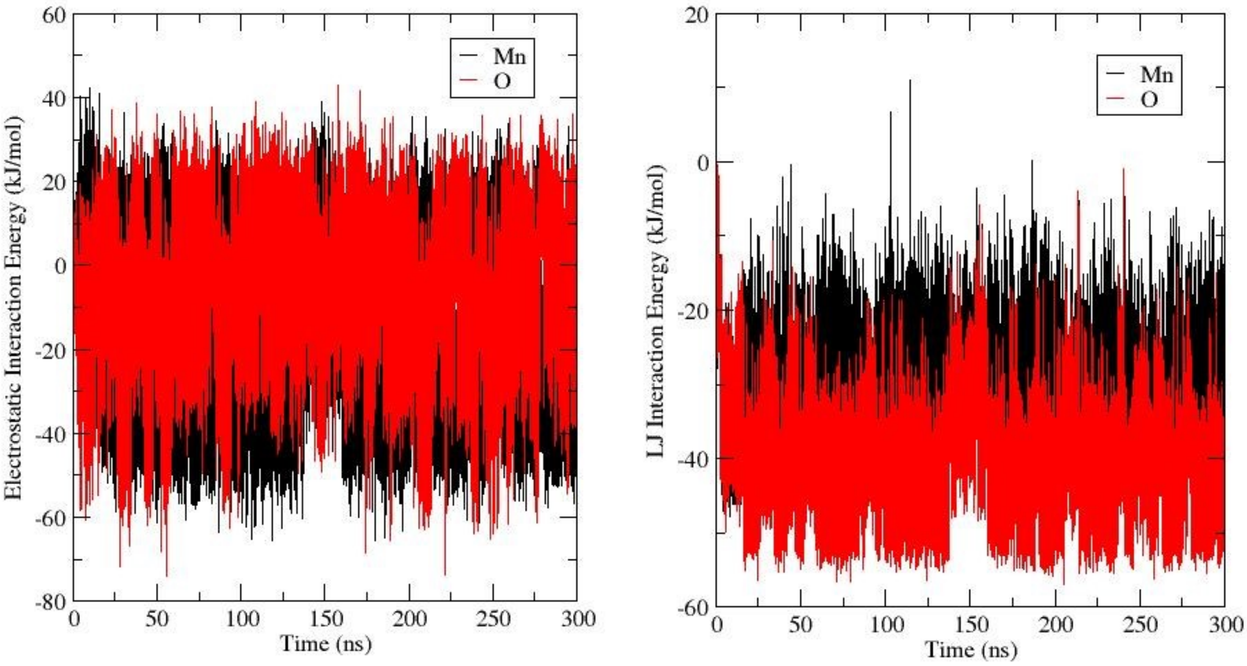

Fig. S3 Interactions of 5'-guanine with Mn and O atoms of Mn_3O_4 surface.

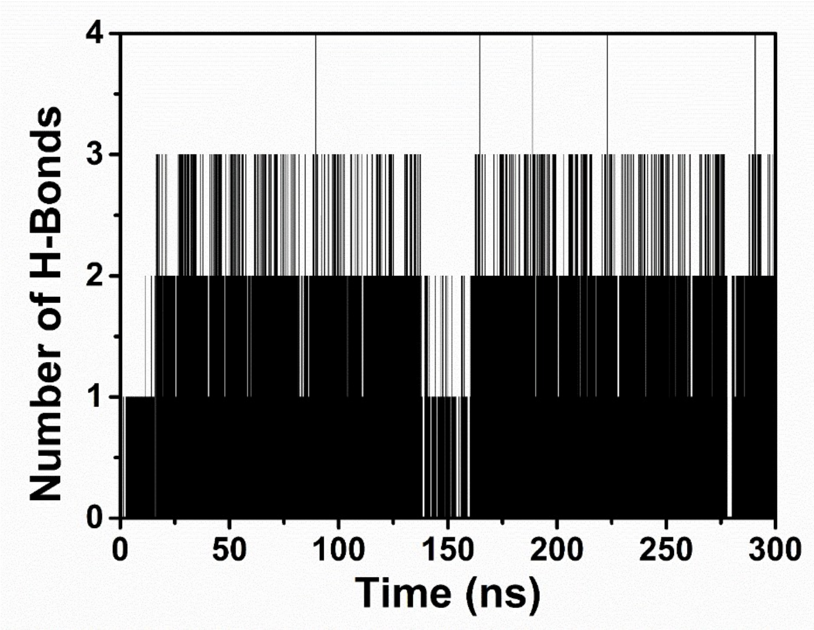

Fig. S4 Number of hydrogen bonds formed between 5'-guanine and 2D Mn_3O_4 surface.

Section S1: Additional Details of simulation

In the present study, the following standard 12-6 LJ potential form was used to describe the non-bonded VdW interactions.

$$V_{LJ}(r_{ij}) = 4\varepsilon_{ij}\left(\left(\frac{\sigma_{ij}}{r_{ij}}\right)^{12} - \left(\frac{\sigma_{ij}}{r_{ij}}\right)^{6}\right)\ldots\ldots\ldots\ldots\ldots\ldots\ldots\ldots\ldots\ldots(1)$$

Following Lorentz-Berthelot combination rules were used to obtain the cross interaction terms.

$$\sigma_{ij} = \frac{1}{2}(\sigma_{ii} + \sigma_{jj})\ldots\ldots\ldots\ldots\ldots\ldots\ldots\ldots\ldots\ldots\ldots\ldots\ldots\ldots(2)$$

$$\varepsilon_{ij} = (\varepsilon_{ii}\varepsilon_{jj})^{\frac{1}{2}}\ldots\ldots\ldots\ldots\ldots\ldots\ldots\ldots\ldots\ldots\ldots\ldots\ldots\ldots(3)$$

Where r is the distance between two particles, ε is the depth of the potential, and σ is the size of the particle. Bonds were described using harmonic potentials. It is noteworthy that during simulation, the v-rescale thermostat was applied separately for the ssDNA, the surface, and the solvent with ions. Parrinello–Rahman barostat was engaged with an isothermal compressibility of 4.5×10^{-5} bar^{-1}. PME method was applied with a tolerance of 10^{-5}, Fourier grid spacing of 0.16 nm and an interpolation order of 4 for the Ewald mesh.

Analysis were carried out using different *gmx* modules and *in house scripts* as described below.

1. Interaction energies were computed using *gmx energy* module.
2. Distance and number of contacts were calculated using *gmx mindist* module. The cut-off distance used was 0.4nm.
3. Number of hydrogen bonds was calculated using *gmx hbond* module, with a cut-off distance of 0.35nm.
4. Radius of gyration was computed using *gmx gyrate* module using following equation.

$$R_g = \left(\frac{\sum_i \|r_i\|^2 m_i}{\sum_i m_i} \right)^{1/2}$$

Where m_i is the mass of the i^{th} particle, and r_i is the distance of the i^{th} particle from centre of mass.

5. RMSD was calculated using *gmx rms* module using the following equation.

$$\mathrm{RMSD}\ (t_1, t_2) = \left[\frac{1}{M} \sum_{i=1}^{N} m_i \|r_i(t_1) - r_i(t_2)\|^2 \right]^{\frac{1}{2}}$$

Where M is the total mass and $r_i(t)$ is the position of atom *i* at time t.

6. IR spectra was obtained from velocity autocorrelation function, using *gmx velacc* module.

Section S2: Bahaviour of multiple ssDNAs on Mn_3O_4 (0 0 1) surface

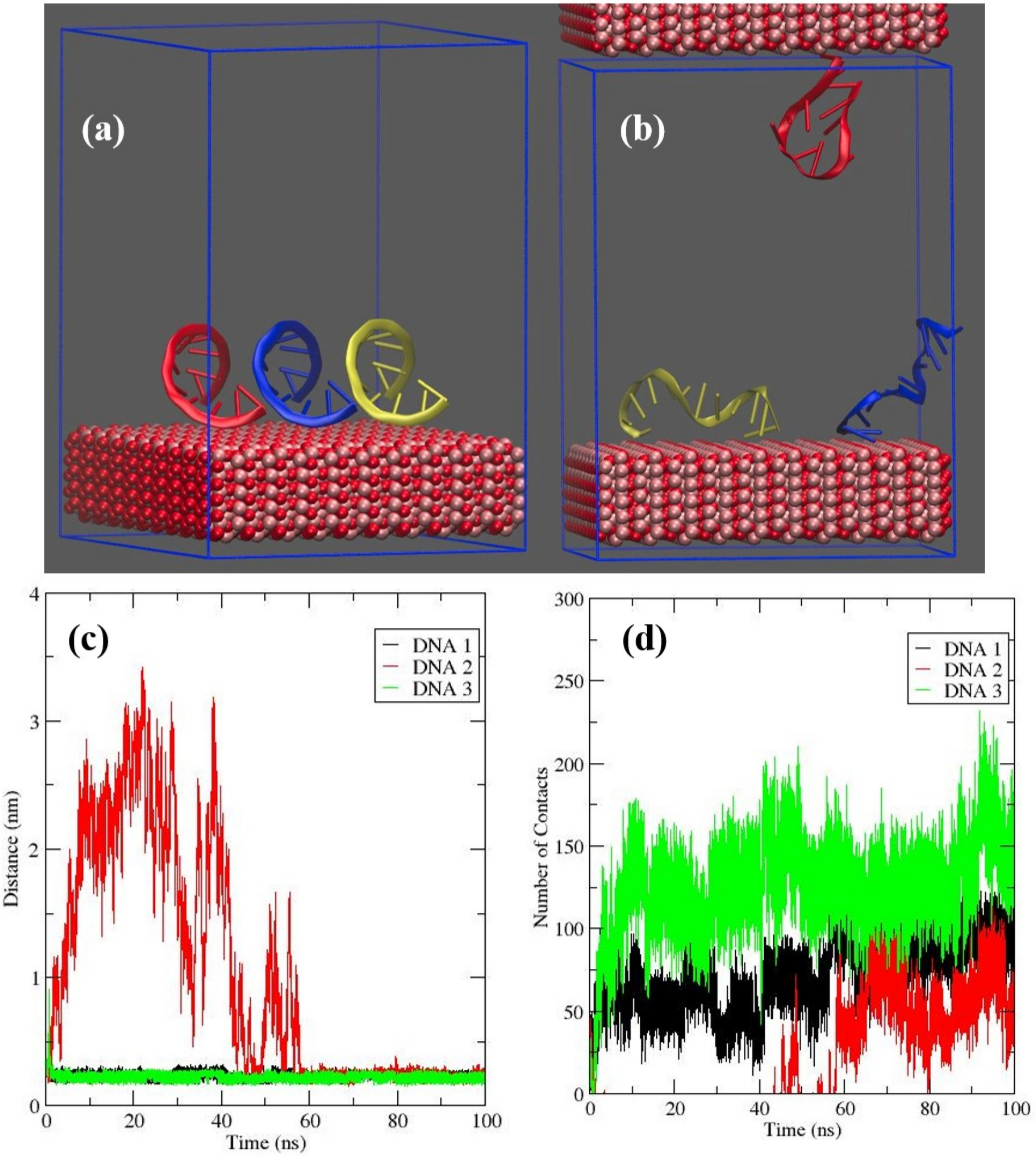

Fig. S5: Snapshot of the system at (a) 0ns and (b) 100ns. DNA segments are presented with colour code: Blue: DNA1, Red: DNA 2, yellow: DNA 3. Surface presented using VdW spheres with colour code: Red: O, Pink: Mn. Water molecules removed for clarity. (c) Minimum distance between ssDNA segments and surface; (d) number of contacts formed between ssDNA segments and surface

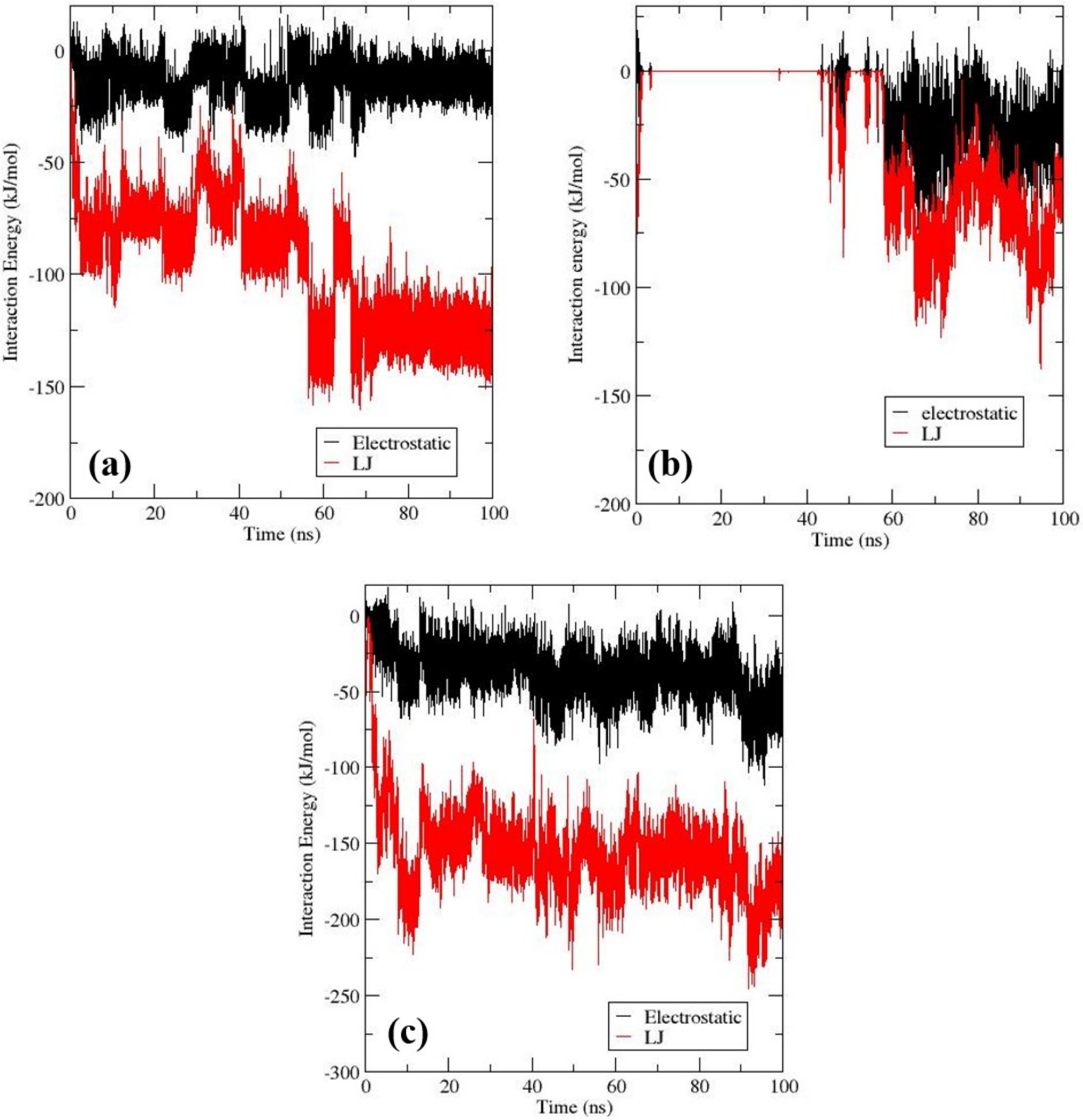

Fig. S6: Interaction energy between Mn_3O_4 surface and (a) DNA 1;(b) DNA 2; and (c) DNA 3

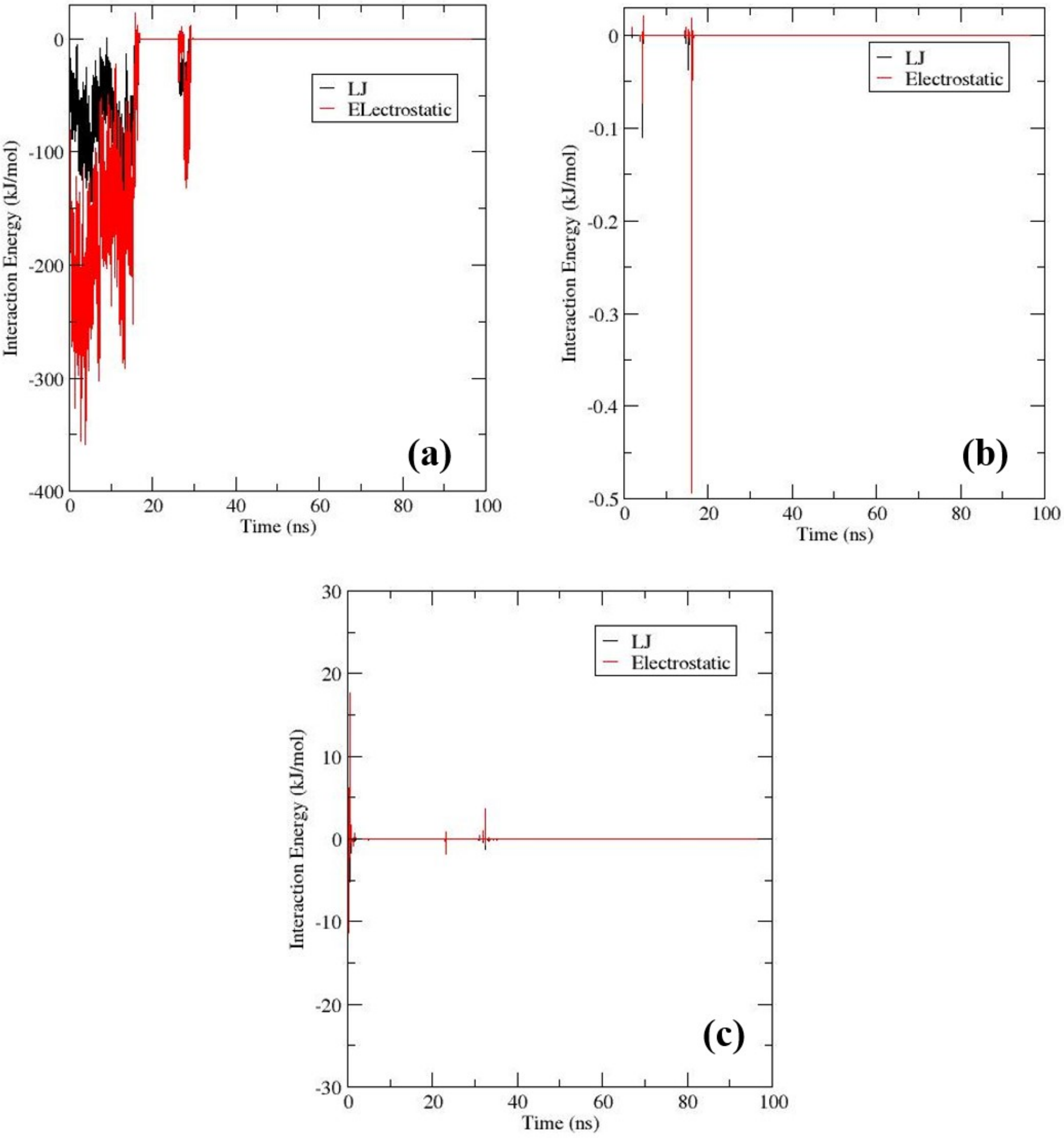

Fig. S7: Interaction energy between (a) DNA 1-DNA 2;(b) DNA 2-DNA 3; and (c) DNA 3-DNA 1

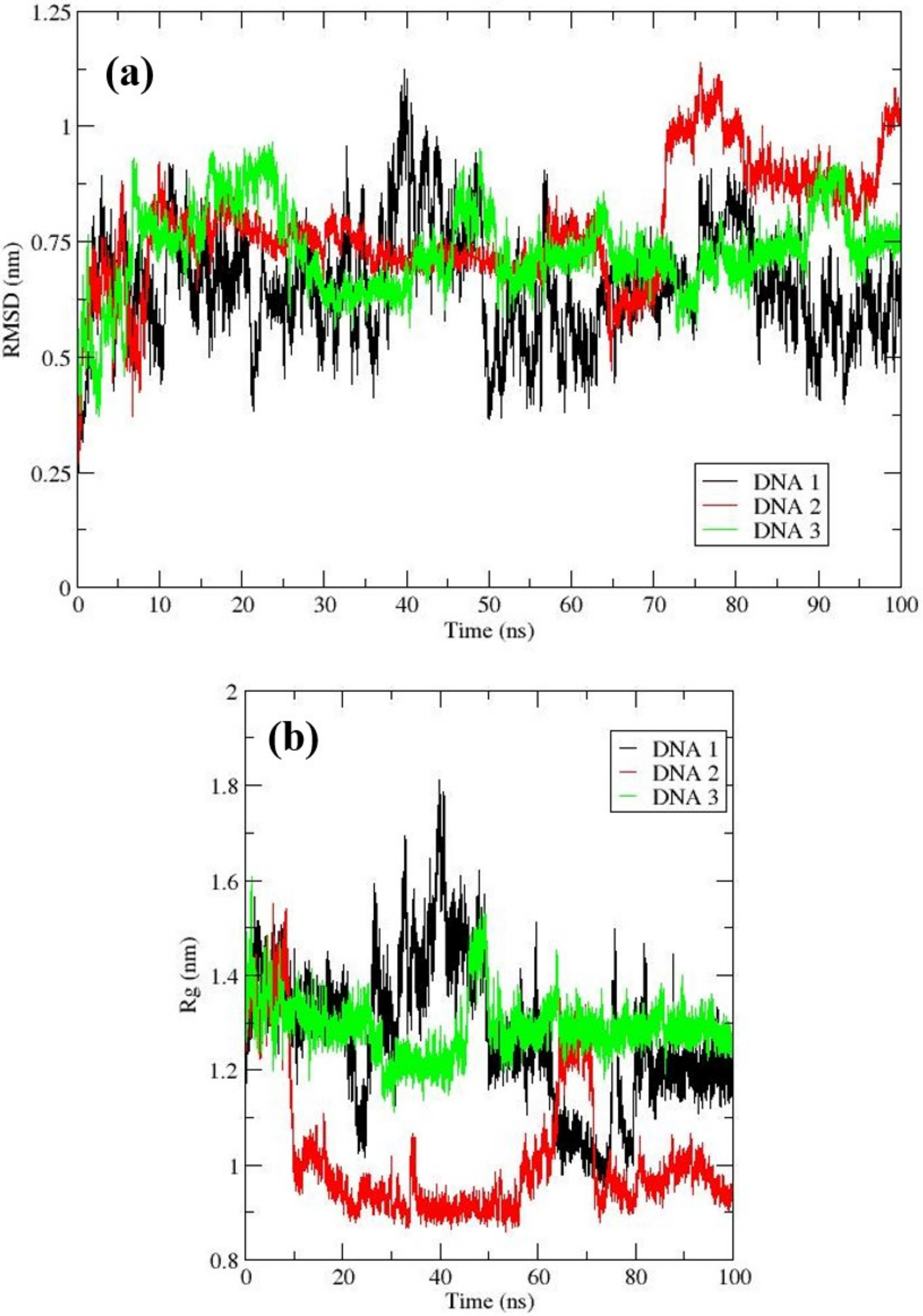

Fig. S8: (a)RMSD and (b) radius of gyration of ssDNA segments

Intending to mimic experimental conditions better, we have run 100ns simulations placing 3 ssDNA segments on Mn_3O_4 (0 0 1) surface. The initial and final snapshots of the system have been shown in Fig. S5(a) and Fig. S5(b). The behaviour of the multiple ssDNA segments were found to be quite similar to the single ssDNA on Mn_3O_4 (0 0 1) surface. All of the ssDNA segments eventually got adsorbed on the surface and 5'-guanine was recorded to be the most interacting nucleotide for all the DNA segments (data not shown). Like the single ssDNA case, the VdW interactions were noticed to be the dominant force behind the adsorption phenomena. The interaction between DNA2 and DNA3 was negligible, but that between DNA1 and DNA 2 has high for the first ~30 ns of the simulation time (Fig. S7(a)). This interaction between DNA2 and DNA1caused the initial desorption of DNA2 from the surface. DNA2 got adsorbed on the surface (on the opposite side) at ~60ns and remained in a steady adsorbed state. On the other hand, the interaction between DNA1 and DNA3 was significant only for an initial few ps of the simulation window but that caused configurational rearrangement of the ssDNA segments, which is reflected in the different temporal evolution of RMSD and R_g of different ssDNA segments (Fig.S8). The observed difference in the surface-ssDNA interaction energy (Fig. S6) was also probably caused by the configurational rearrangement of the ssDNA molecules due to the proximity of the other ssDNAs. However, the surface-DNA interaction energy was found to be higher for all ssDNA segments (at their adsorbed state) than that in the case of single ssDNA. Hence, we can comment that the presence of multiple DNA promotes the adsorption phenomena.

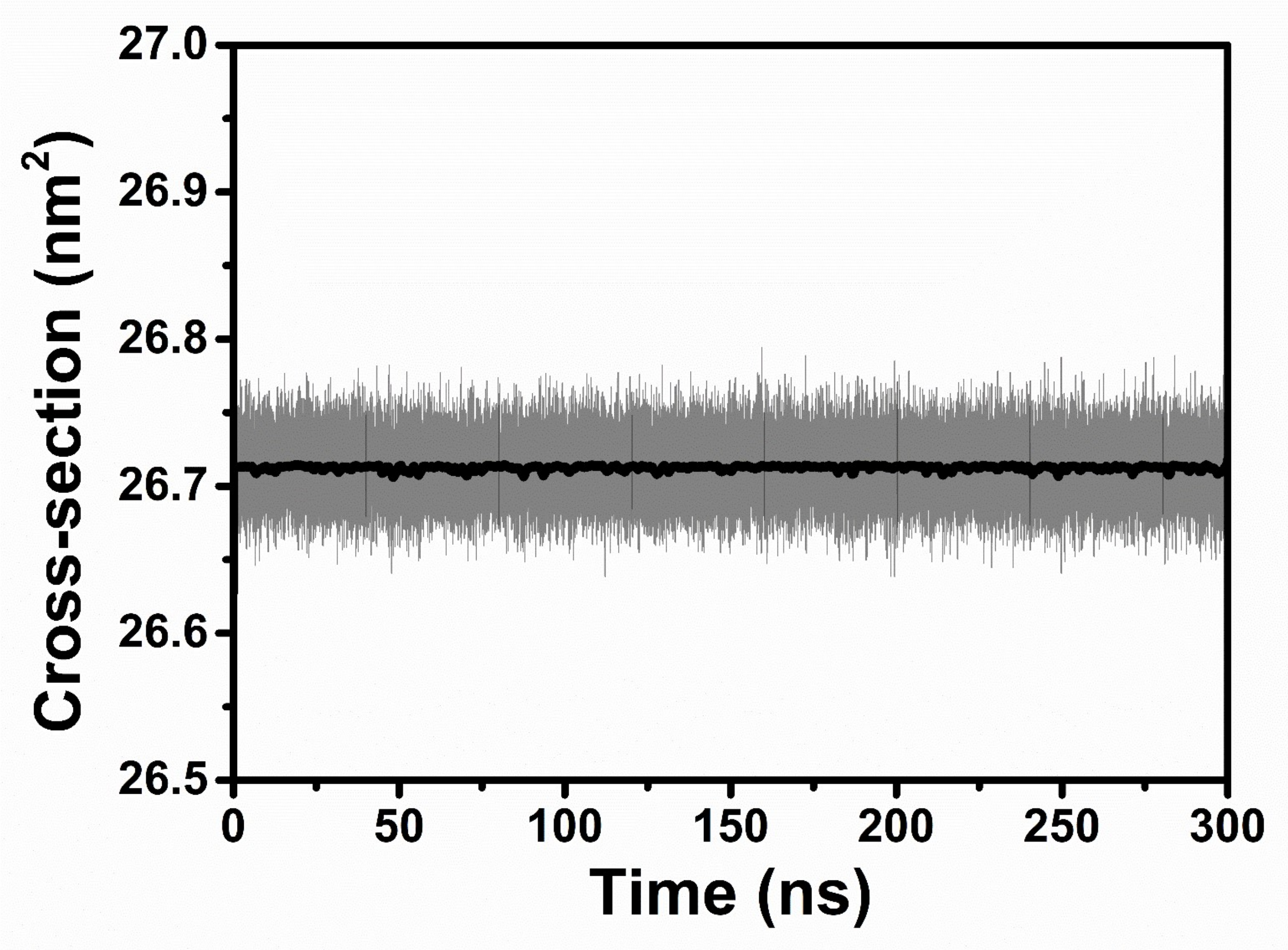

Fig. S9: Cross-sectional area of the simulation box during production run.

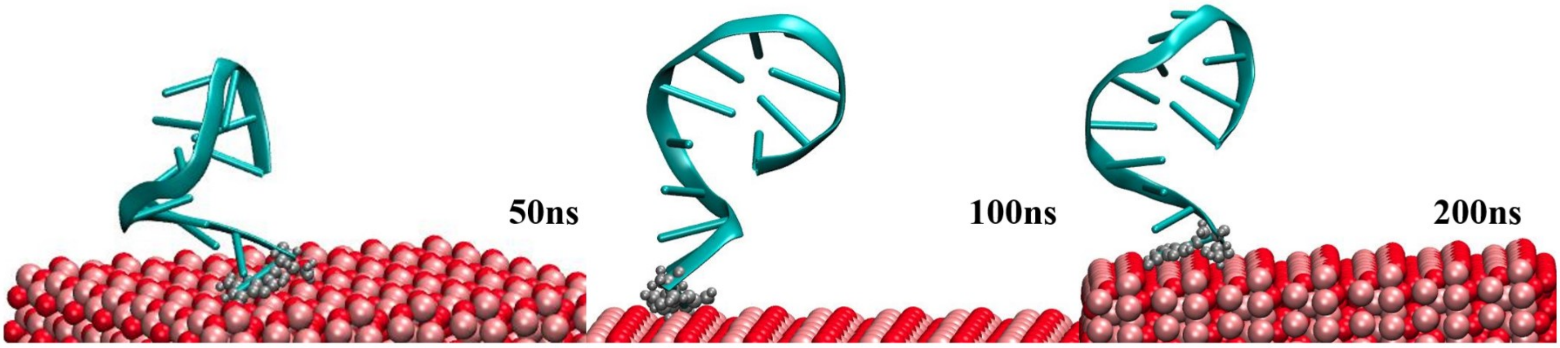

Fig. S10: Snap-shots of the system at different time points. The surface is shown in VdW representations, with colour code: Mn: Pink, O: Red. 5’-guanin is shown in grey spheres. Water molecules and ions are stripped for clarity.

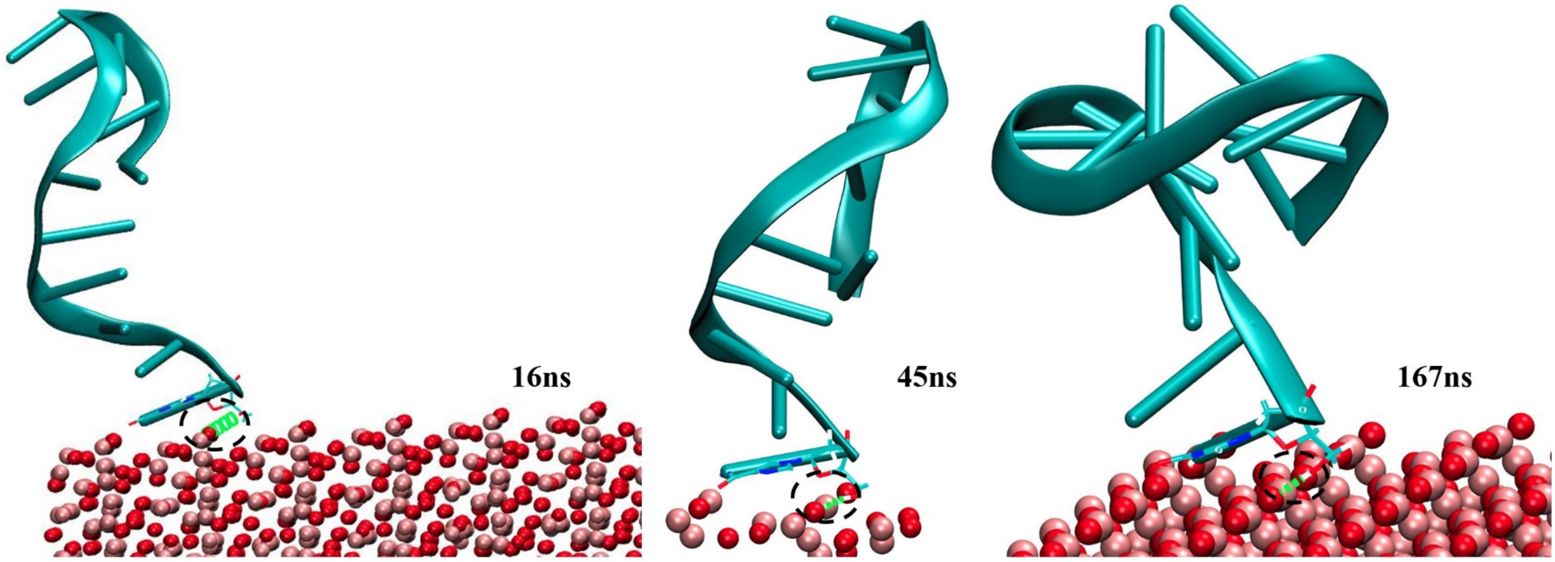

Fig. S11: Snap-shots of the system at different time points, where hydrogen bonds formed between ssDNA and Mn_3O_4 are shown in green dashed line. The surface is shown in VdW representations, with colour code: Mn: Pink, O: Red. 5’-guanin is shown in grey spheres. Water molecules and ions are stripped for clarity.

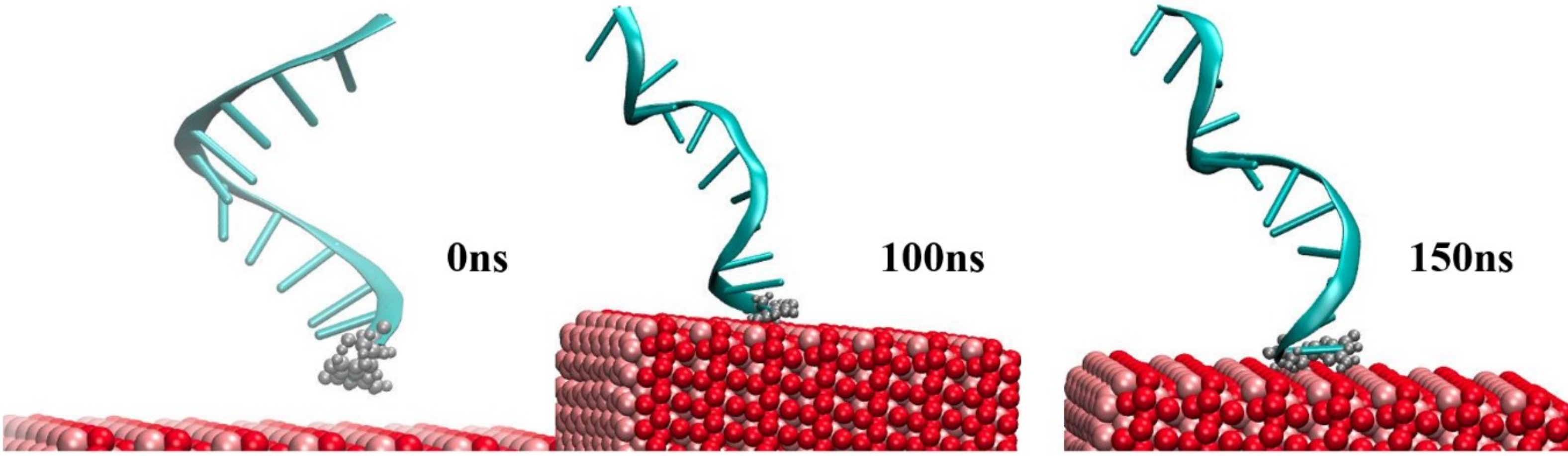

Fig. S12: Snap-shots of the system, where ssDNA was initially perpendicular to the surface (5’end was in proximity to the surface) at different time points. The surface is shown in VdW representations, with colour code: Mn: Pink, O: Red. 5’-guanin is shown in grey spheres. Water molecules and ions are stripped for clarity.

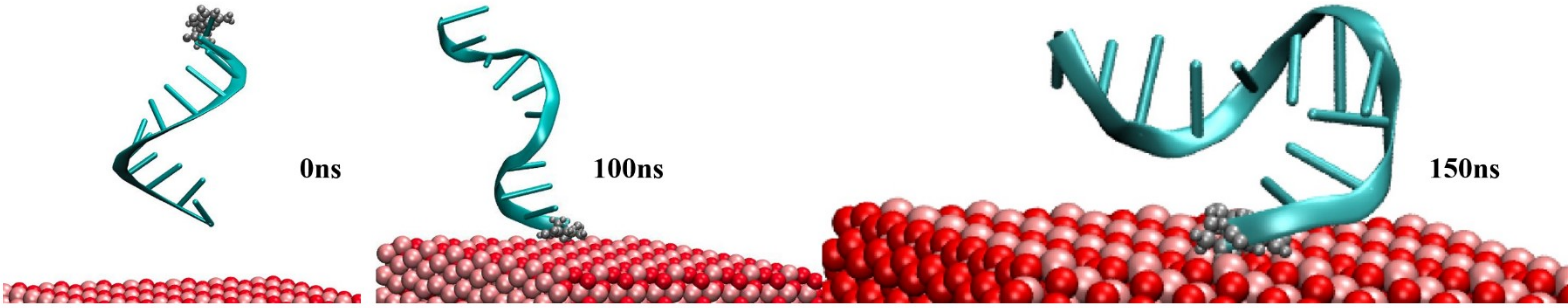

Fig. S13: Snap-shots of the system, where ssDNA was initially perpendicular to the surface (5’end was away from the surface) at different time points. The surface is shown in VdW representations, with colour code: Mn: Pink, O: Red. 5’-guanin is shown in grey spheres. Water molecules and ions are stripped for clarity.

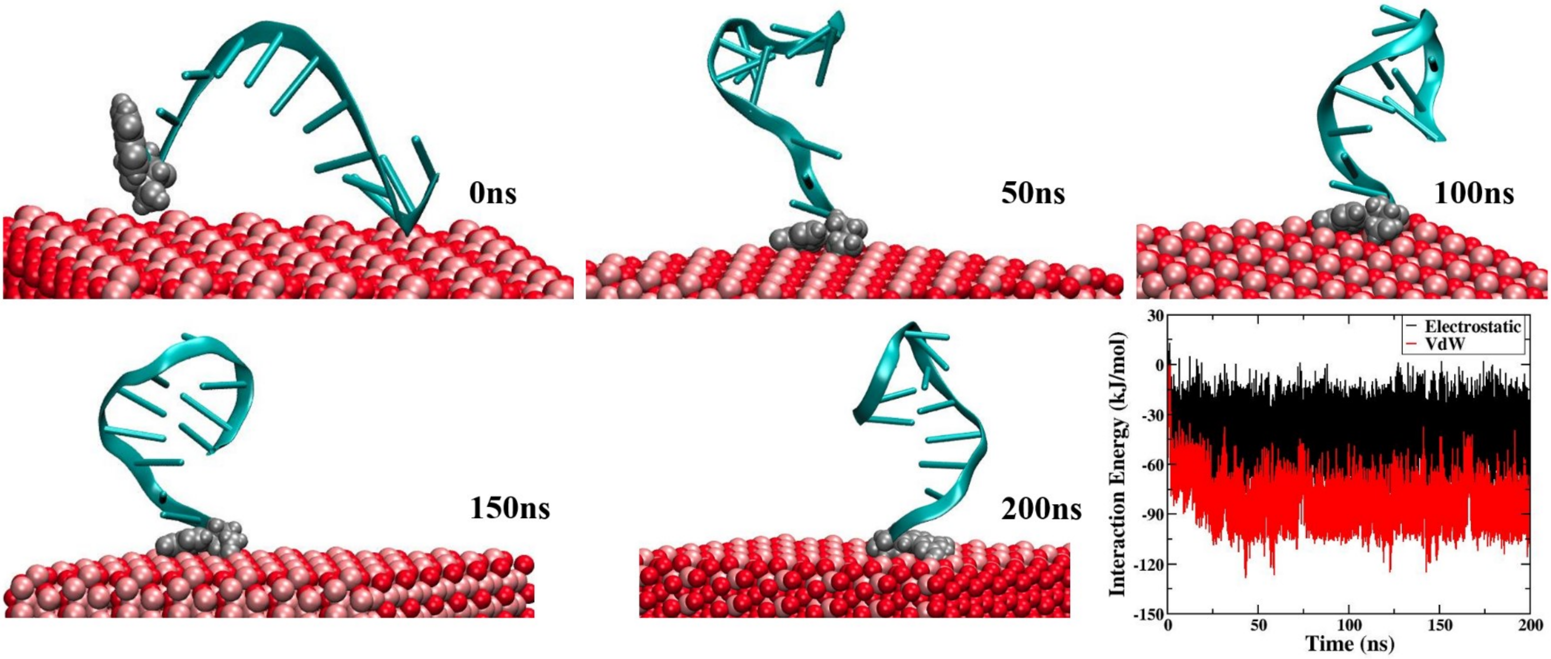

Fig. S14: snapshots of the system with 100mM salt concentration at various time points. ssDNA-surface interaction energies are also plotted. The surface is shown in VdW representations, with colour code: Mn: Pink, O: Red. 5’-guanin is shown in grey spheres. Water molecules and ions are stripped for clarity.

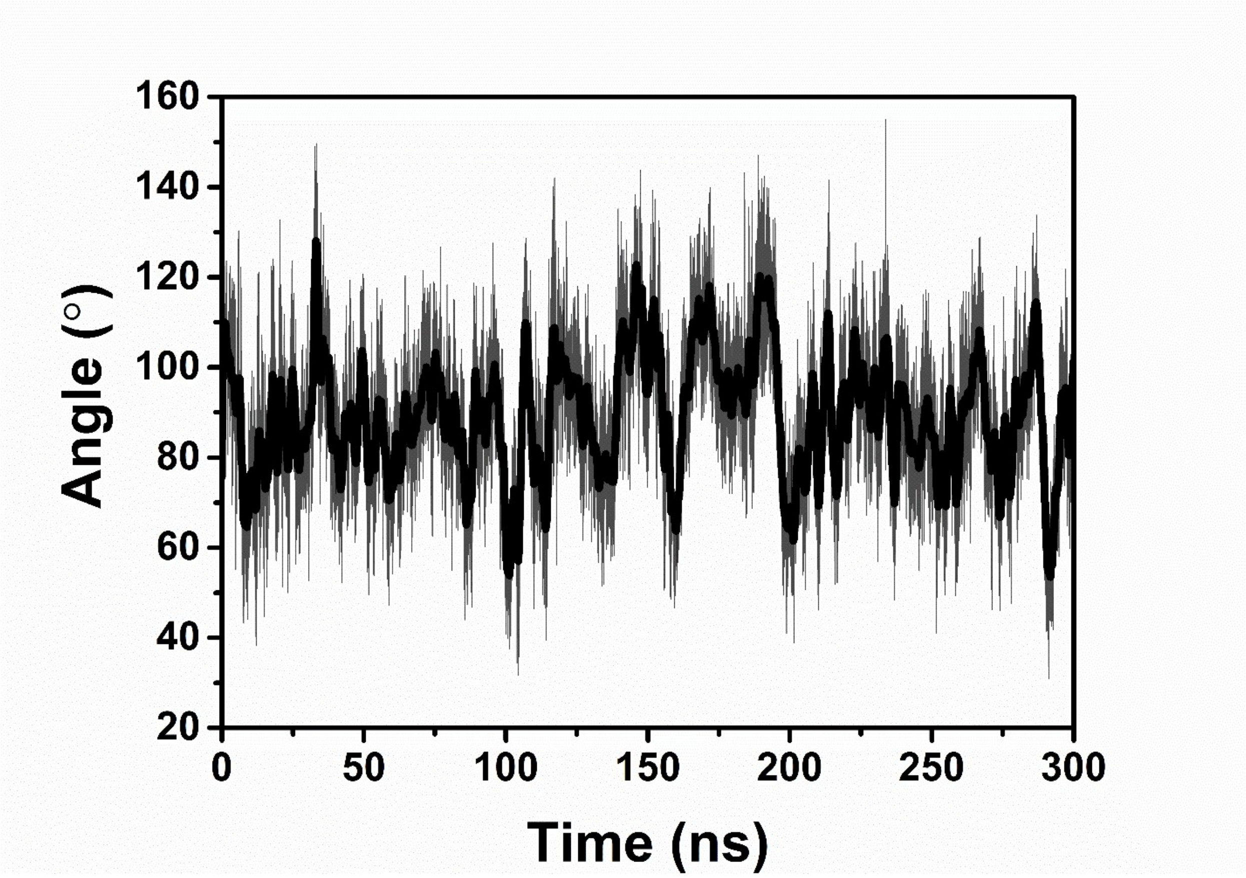

Fig. S15: Temporal variation of the angle between the dipole moment of ssDNA and the dipole moment of Mn_3O_4 slab.

Supplementary Table list

Table Sl 1: Primer list for RT-LAMP reaction.

Sl No.	Primer name	5'-3' Sequences
01	Covid-19C-LOOP-F	TTTTTGATGAAACTGTCTATTGGTCATAGTACTACAG
02	Covid-19C-F3	GCCATTAGTGCAAAGAATAGAG
03	Covid-19C LOOP-B	GGCACAACATGTTAAAAACTGTTTATAGTGATGTAG
04	Covid-19C-BIP	TGTAGTAATTGGAACAAGCAAATTCTATGGTGGCCAACCCATAAGGTGAGGG
05	Covid-19C-B3	GGCATGGCTCTATCACATTTAGG
06	Covid-19C-FIP	TAGCTCCTCTAGTGGCGGCTATTGCACCGTAGCTGGTGTCTC

Table SI 2: Primer list used for PCR amplification during in-vitro transcription.

Sl No.	**Primer name**	**5'-3' Sequences**
01	IVT-ORF-Forward	TAATACGACTCACTATAGGGACTC
01	IVT-ORF-Reverse	TAATTCTAAGCATGTTAGGCATGG

Table: Sl 3: Sequence of DNA template for in-vitro transcription.

Sl No.	**5'-3' Sequences**
01	**5'*TAATACGACTCACTATAGG***GACTCAAATGAATCTTAAGTATGCCATTAGTGCAAAGAATAGAGCTCGCACCGTAGCTGGTGTCTCTATCTGTAGTACTATGACCAATAGACAGTTTCATCAAAAATTATTGAAATCAATAGCCGCCACTAGAGGAGCTACTGTAGTAATTGGAACAAGCAAATTCTATGGTGGTTGGCACAACATGTTAAAAACTGTTTATAGTGATGTAGAAAACCCTCACCTTATGGGTTGGGATTATCCTAAATGTGATAGAGCCATGCCTAACATGCTTAGAATTA**3'** *Bold italic letters indicate T7 RNA polymerase promoter sequence.